Author/s:
Johnson, P;Davies, S;Hogendoorn, H

Title:
Motion extrapolation in the High-Phi illusion: Analogous but dissociable effects on perceived position and perceived motion

Date:
2016-12-01

Citation:
Johnson, P., Davies, S. & Hogendoorn, H. (2016). Motion extrapolation in the High-Phi illusion: Analogous but dissociable effects on perceived position and perceived motion. Journal of Vision, 20 (13), pp.1-14. https://doi.org/10.1167/jov.20.13.8.

Persistent Link:
https://hdl.handle.net/11343/272484

Motion extrapolation in the High-Phi illusion: Analogous but dissociable effects on perceived position and perceived motion

Philippa Johnson Melbourne School of Psychological Sciences, Parkville, Victoria, Melbourne, Australia

Sidney Davies Melbourne School of Psychological Sciences, Parkville, Victoria, Melbourne, Australia

Hinze Hogendoorn Melbourne School of Psychological Sciences, Parkville, Victoria, Melbourne, Australia

A range of visual illusions, including the much-studied flash-lag effect, demonstrate that neural signals coding for motion and position interact in the visual system. One interpretation of these illusions is that they are the consequence of motion extrapolation mechanisms in the early visual system. Here, we study the recently reported High-Phi illusion to investigate whether it might be caused by the same underlying mechanisms. In the High-Phi illusion, a rotating texture is abruptly replaced by a new, uncorrelated texture. This leads to the percept of a large illusory jump, which can be forward or backward depending on the duration of the initial motion sequence (the inducer). To investigate whether this motion illusion also leads to illusions of perceived position, in three experiments we asked observers to localize briefly flashed targets presented concurrently with the new texture. Our results replicate the original finding of perceived forward and backward jumps, and reveal an illusion of perceived position. Like the observed effects on illusory motion, these position shifts could be forward or backward, depending on the duration of the inducer: brief inducers caused forward mislocalization, and longer inducers caused backward mislocalization. Additionally, we found that both jumps and mislocalizations scaled in magnitude with the speed of the inducer. Interestingly, forward position shifts were observed at shorter inducer durations than forward jumps. We interpret our results as an interaction of extrapolation and correction-for-extrapolation, and discuss possible mechanisms in the early visual system that might carry out these computations.

Introduction

A wide range of visual illusions show that motion and position signals interact in the visual system. Perhaps the best known is the flash-lag effect, in which a static object that is flashed alongside a moving object is perceived to lag behind the moving object (Hubbard, 2014; Nijhawan, 1994; Nijhawan, 2008). In the related Fröhlich effect, the perceived position of the initial appearance of a moving object is shifted along its trajectory (Fröhlich, 1924). When features of a moving object, such as its color or size, abruptly change, those changes are perceived to occur further along the trajectory than they physically occur (Cai & Schlag, 2001), and when a moving object reverses direction, the object is perceived to reverse well before its true reversal point (Sinico, Parovel, Casco, & Anstis, 2009). Similarly, when an object is briefly flashed on a texture when that texture reverses direction, the perceived position of that object is likewise shifted back along the trajectory of the texture (the flash-grab effect; Cavanagh & Anstis, 2013). A flash presented alongside a moving texture is perceived shifted in the direction of motion of that texture (the flash-drag effect; Whitney & Cavanagh, 2000), and a patch containing a moving texture itself appears shifted in the direction of its internal motion (Anstis, 1989; De Valois & De Valois, 1991; Ramachandran & Anstis, 1990).

A relatively recent addition to this list is the High-Phi illusion, in which a rotating random texture is suddenly replaced by an entirely new random texture (Wexler, Glennerster, Cavanagh, Ito, & Seno, 2013). Strikingly, if the rotating texture (the inducer) is presented for more than ~ 110 ms, the transient evokes a strong

Citation: Johnson, P., Davies, S., & Hogendoorn, H. (2020). Motion extrapolation in the High-Phi illusion: Analogous but dissociable effects on perceived position and perceived motion. *Journal of Vision*, *20*(13):8, 1–14, https://doi.org/10.1167/jov.20.13.8.

https://doi.org/10.1167/jov.20.13.8 Received February 11, 2020; published December 9, 2020 ISSN 1534-7362

illusion of coherent motion: a sharp jump backward along the direction of rotation, even though the two textures are uncorrelated. Interestingly, the authors note that at short inducer durations (~ 20–100 ms) the jump is forward along the initial motion trajectory, rather than backward. Wexler et al. argue that the replacement of the inducer with an uncorrelated noise texture provides motion energy in all directions, which is interpreted as a jump with maximum detectable velocity. They propose that at short inducer durations the inducer motion acts as a motion prime, causing the ambiguous transient to be interpreted as a forward jump. In contrast, after a longer inducer duration, the ambiguous transient is interpreted as a backward jump, due to the motion aftereffect. Similar time-dependent effects have been found in research into motion priming (Kanai & Verstraten, 2005; Pinkus & Pantle, 1997; Priebe, Churchland, & Lisberger, 2002). However, only a handful of studies have investigated the High-Phi illusion since its first description (e.g. Fabius, Fracasso, Nijboer, & Van der Stigchel, 2019; Fabius, Fracasso, & Van der Stigchel, 2016), and the underlying neural mechanisms remain unclear.

In contrast, the flash-lag effect has been the subject of intense investigation and debate since it was first interpreted by Nijhawan as evidence for visual motion extrapolation (Nijhawan, 1994). Although several other explanations have been proposed (see Hubbard, 2014; Maus, Khurana, & Nijhawan, 2010 for reviews), convergent behavioral, computational, and neuroimaging evidence continues to support the existence of motion extrapolation mechanisms in the visual system, and their role in the flash-lag and related illusions (Hogendoorn, 2020; Nijhawan, 1994; Nijhawan, 2008). In this interpretation, motion signals interact with position signals to shift the perceived position of moving objects in the direction of motion (Eagleman & Sejnowski, 2007), proportional to the speed of motion (Nijhawan, 1994), potentially serving to counteract neural processing delays. One key feature of this interpretation is that motion extrapolation is established very rapidly, and starts very early in the visual system. Motion signals have been shown to be available to influence position signals within less than 1 ms (Nijhawan, 2008; Westheimer & McKee, 1977), and neural extrapolation mechanisms have been identified as early as the retina (Berry, Brivanlou, Jordan, & Meister, 1999; Hosoya, Baccus, & Meister, 2005; Schwartz, Taylor, Fisher, Harris, & Berry, 2007). In humans, evidence from electroencephalogram (EEG; Hogendoorn, Verstraten, & Cavanagh, 2015), functional magnetic resonance imaging (fMRI; Schneider, Marquardt, Sengupta, Martino, & Goebel, 2019), and behavioral studies (van Heusden, Harris, Garrido, & Hogendoorn, 2019) converges to indicate that position information is influenced by motion signals even before that information reaches primary visual cortex.

A second key feature of the motion extrapolation interpretation is that when the visual system over-extrapolates (for example, because a moving object unexpectedly disappears), the erroneously extrapolated signal is overwritten by a retroactive "correction-for-extrapolation" signal (Nijhawan, 2008; Shi & Nijhawan, 2012) such that the overshoot is not consciously perceived (Eagleman & Sejnowski, 2000). This correction signal is triggered by the disappearance of the object; when that disappearance is made less salient, observers do perceive the object to overshoot (Maus & Nijhawan, 2006; Maus & Nijhawan, 2008; Maus & Nijhawan, 2009; Shi & Nijhawan, 2012). The same mechanism was also recently shown to play a role in the flash-grab illusion (Blom, Liang, & Hogendoorn, 2019): when an object is flashed on a moving background that suddenly changes direction to an orthogonal direction, the object is not only "grabbed" in the direction of new motion (as demonstrated in the initial report of the flash-grab effect; Cavanagh & Anstis, 2013), but also "pulled" back along the initial motion vector, consistent with a mechanism correcting for over-extrapolation (Blom et al., 2019). Together, predictive extrapolation mechanisms and "postdictive" (Eagleman, 2008; Eagleman & Sejnowski, 2000) correction-for-extrapolation mechanisms allow the visual system to predict the real-time position of a moving object despite neural delays, and to overwrite that prediction if it turns out wrong (Eagleman, 2008).

This interplay between forward extrapolation mechanisms and backward corrective mechanisms for position representations closely mirrors the pattern of effects observed for motion in the High-Phi illusion. After brief inducers, transients induce forward motion percepts, just as short motion sequences are sufficient to calculate motion extrapolation signals for position (Nijhawan, 2008; Westheimer & McKee, 1977). Conversely, after longer inducers, transients induce backward motion percepts, just like correction-for-extrapolation mechanisms induce shifts in position backward along the motion trajectory when a moving object disappears. Although there are numerous paradigmatic and methodological differences (both spatial and temporal) between these empirical results, this analogous pattern of effects led us to ask whether the illusory motion perceived in the High-Phi illusion might be caused by the same extrapolation and correction mechanisms that influence the perceived position of objects in or near motion.

Here, we investigate the hypothesis that the High-Phi illusion is caused by the same motion extrapolation mechanisms that we have previously argued underlie the flash-lag, flash-grab, and related position illusions. To do this, we adapt the traditional High-Phi illusion (Wexler et al., 2013) by additionally asking observers to localize briefly flashed targets presented concurrently with the transient new texture that induces

illusory jumps. If those jumps are caused by motion extrapolation signals, then those same signals should influence the perceived position of the flashed target, as in the flash-grab effect. In three experiments, we show that indeed the High-Phi illusion induces not only an illusory motion signal (the jump), but also an illusory position shift. Furthermore, both jumps and position shifts are backward along the trajectory for long inducer durations, and forward along the trajectory for short inducer durations. However, the two effects peak at different inducer durations, with maximal forward mislocalization evident at shorter inducer duration ($\sim$ 20 ms) than maximal forward jumps ($\sim$ 100 ms). Additionally, this effect scales with speed of rotation of the inducer, with faster speeds causing greater jumps and position shifts forward or backward along the motion path. This pattern of results is consistent with the interpretation that the High-Phi effect is a manifestation of the same extrapolation and correction mechanisms that are involved in the flash-lag and related illusions.

Experiment 1

Method

Observers

Thirty observers (23 women and 7 men) aged between 19 and 42 years (M = 24.37, SD = 5.39) took part in the study. Observers were right-handed, proficient in English, and had normal or corrected-to-normal vision. This study was approved by the local human research ethics committee of the Melbourne School of Psychological Sciences and conducted in accordance with the guidelines in the Declaration of Helsinki. Observers were compensated for their participation.

Stimulus

Stimuli were presented on an ASUS ROG PG258 monitor (ASUS, Taipei, Taiwan) with a resolution of 1920 $\times$ 1080 running at 200 Hz. The monitor was connected to a HP EliteDesk 800 PC running MATLAB R2017b (Mathworks, Natick, MA, USA) with PsychToolbox version 3.0.14 extensions (Brainard, 1997). Monitor output was linearized, and the luminance of the background was half of the maximum monitor output, with stimuli presented at maximum contrast. Observers viewed the stimulus from a chinrest at a distance of approximately 50 cm from the monitor. The experiment was conducted in a quiet, dark room.

The stimulus was based on the stimulus presented by Wexler et al. (2013) and consisted of a rotating annulus surrounding a white central fixation dot, presented on a uniform 50% grey background (Figure 1). The annulus had an outer radius of 9.8 degrees of visual angle (dva) and an inner radius of 4.9 dva, and contained a full-contrast grayscale 1/f noise texture rotating at 200 degrees rotation per second. New noise textures were randomly generated for each trial.

On each trial, a static annulus was presented for 1000 ms, after which it rotated in a randomly chosen direction (either clockwise or anti-clockwise) for one of 22 possible durations (0, 5, 10, 15, 20, 25, 30, 35, 40, 45, 50, 75, 100, 125, 150, 175, 250, 325, 500, 750, 1000, or 1500 ms). We call this rotating pattern the inducer. The annulus was then replaced by a sequence of seven new uncorrelated random textures presented in succession at 15 ms per texture. This choice of transient was motivated by initial pilot experiments suggesting that (as reported by Wexler et al. 2013), a transient consisting of multiple successive textures produced a more consistent illusion. The final texture was presented for an additional 1000 ms, after which the stimulus disappeared and the observer could provide a response.

Task

Trials were presented in two types of blocks:

In *Jump* blocks, after the stimulus disappeared, observers were instructed to report (2AFC) the direction of any perceived jump in the annulus, as in the original report of the High-Phi illusion (Wexler et al., 2013).

In *Position* blocks, a red disc (radius 0.98 dva) was presented for 15 ms, superimposed on the annulus at 8.4 dva away from fixation in one of three possible locations (160, 180, or 200 degrees of polar angle away from vertical). This red disc was presented concurrently with the first of the seven transients following the inducer. At the end of the trial, the mouse cursor was replaced by an identical red disc, and observers used the mouse to indicate the position in which they perceived the red disc during the trial.

Procedure

Each observer completed four Jump blocks followed by four Position blocks, each of which consisted of six repetitions of each inducer duration for a total of 132 trials per block. Trials were presented in random order within each block.

Results

Observer responses in the Jump blocks were collapsed across rotation directions. We then calculated the proportion of jumps perceived in the direction of inducer motion, as a function of inducer duration, before aggregating across all 30 observers.

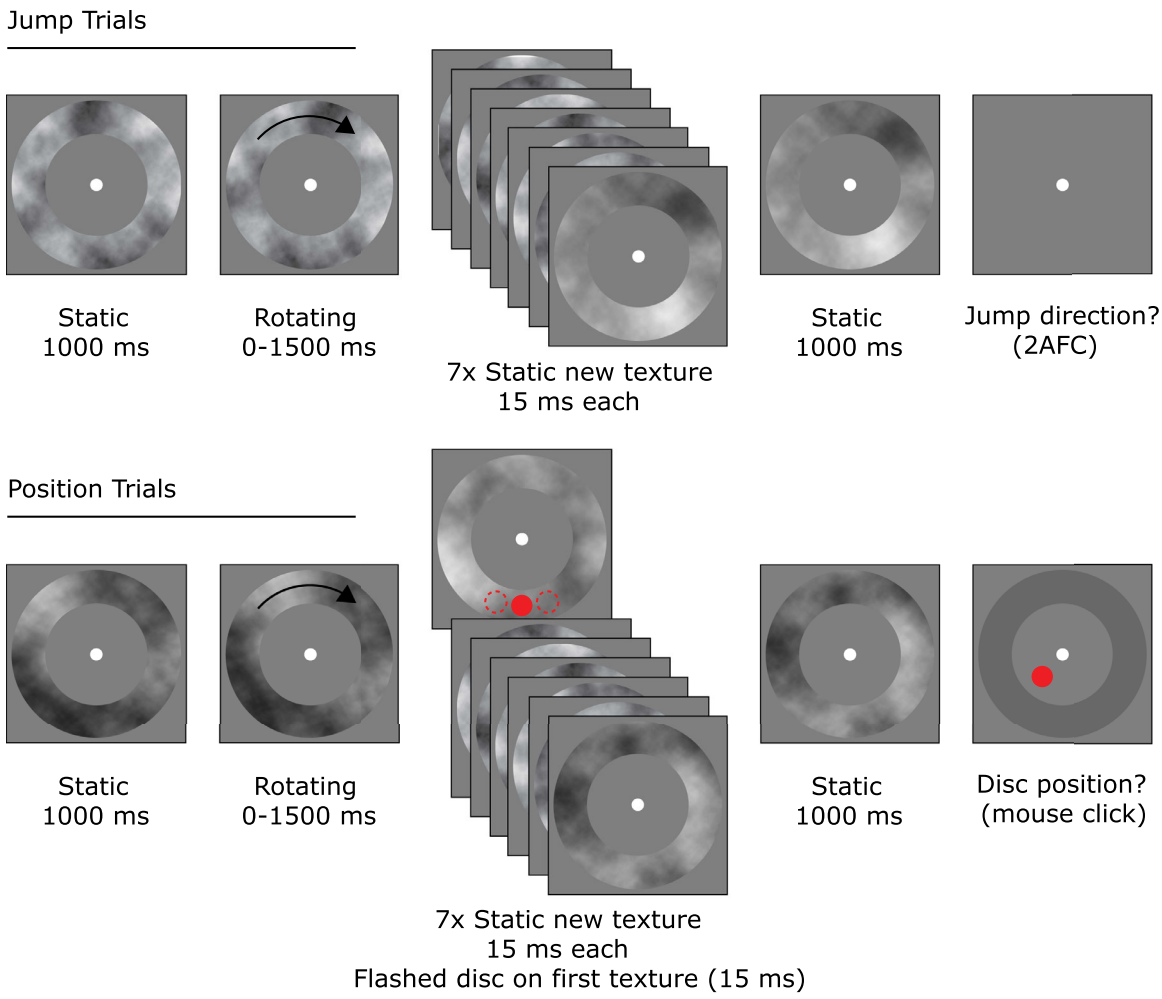

Figure 1. Experiment 1 stimulus and trial sequence. Observers completed trials in two different blocks: Jump blocks and Position blocks. In both cases, they viewed an annulus that started to rotate for a variable duration. The rotating annulus was then replaced by a series of seven brief transients as per Wexler et al. (2013). In Jump blocks, observers reported the direction in which the annulus was perceived to jump (clockwise or counter-clockwise; top sequence). In Position blocks, observers used the mouse to report the position of a red disc that was briefly flashed on top of the first transient in one of three possible locations (bottom sequence).

In the Position blocks, we calculated mislocalization on each trial as the polar difference between the reported position and the physical position of the presented disc, taking mislocalization in the direction of the inducer as positive. We then calculated mean mislocalization as a function of inducer duration, collapsing across rotation directions, and finally aggregating across all 30 observers.

Results for both Jump and Position blocks are shown in Figure 2. For clarity, data are shown on both linear (left panel) and logarithmic abscissas (right panel). For the Jump trials (shown in red), the pattern of results is consistent with results reported by Wexler et al. (2013). Importantly, the pattern of results on Position trials shows a qualitatively similar pattern of results, characterized by forward mislocalization at short inducer durations and backward mislocalization at longer inducer durations.

To test the robustness of this pattern, we tested both proportion of perceived jumps and mean mislocalization against zero at each individual time point, correcting for multiple comparisons by Bonferroni correction. For perceived jumps, the results reveal a significant pattern of forward jumps at short inducer duration (30–100 ms) and backward jumps at longer durations (325–1500 ms). For mislocalization, the backward shift was significant for 150 ms and 500 to 1500 ms, but did not reach significance for the forward shift at short inducer durations.

Because Jump trials and Position trials were measured on different scales, we could not compare individual time points directly. In order to evaluate whether inducer duration affected perceived motion and perceived position similarly, we fitted a double logistic function to each. This function was defined as the difference of two logistic functions, such that it

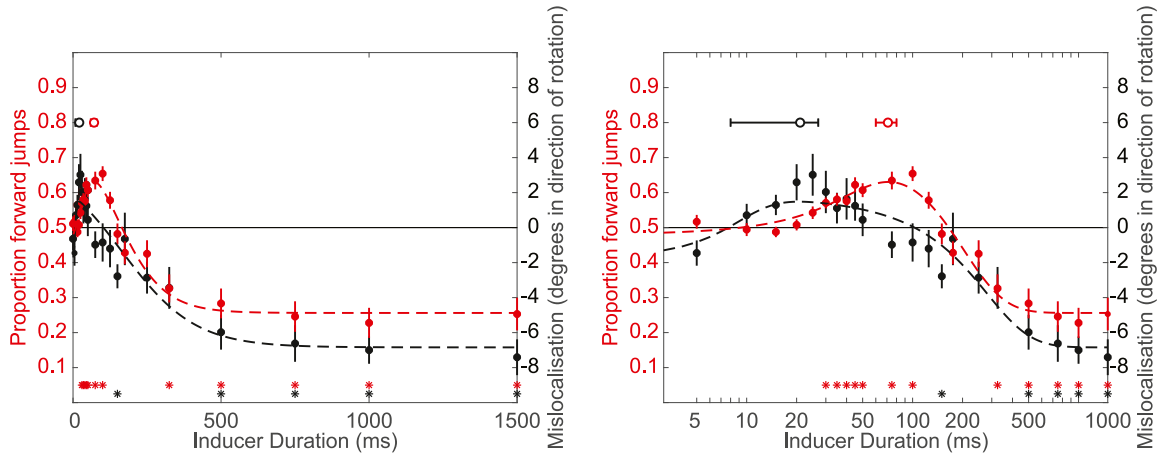

Figure 2. Results Experiment 1. Each panel shows the proportion of jumps reported in the direction of motion in Jump trials (red markers; left vertical axis), and the mean mislocalization in the direction of motion in Position trials (black markers; right vertical axis). In both panels, results are plotted as a function of inducer duration, using a linear abscissa in the left panel and a logarithmic abscissa in the right panel. Error bars indicate standard errors of the mean across 30 observers. Asterisks below the plots indicate individual datapoints that are significantly different from zero (two-tailed *t*-test, $P < 0.05$, Bonferroni corrected). Datapoints are fitted with a double-logistic function (dashed lines; see text). For both functions, we calculated the inducer duration associated with maximum effect in the forward direction (indicated in the plots by filled circles above the plots. Horizontal lines extending from these circles indicate bootstrapped 95% confidence intervals, showing that the High-Phi maximally affects motion and position at different inducer durations.

could accommodate a rise from baseline to a positive peak, followed by a drop from that peak to reach a negative asymptote:

$$f\ (t) = \frac{b_1}{1 + e^{-c_1(t-t_1)}} - \frac{b_2}{1 + e^{-c_2(t-t_2)}}$$

In each of the two terms, b_i is a constant that scales the amplitude of that logistic function, c_i is a constant that determines the slope of that logistic function, and t_i is the horizontal offset of that logistic function (i.e. the inducer duration at which it reaches half its maximum amplitude).

Optimal (i.e. minimal sum of squared error) fits to the data are plotted as dashed lines in Figure 2. To estimate the respective inducer durations at which we observed the greatest proportion of forward jumps and maximal forward mislocalization, we took the inducer duration corresponding to the maxima of the fitted functions, indicated as open circles above the plots in Figure 2, with horizontal error bars indicating bootstrapped 95% confidence intervals (CIs). These confidence intervals were obtained by generating 10,000 new datasets from the original dataset, randomly drawing the same number of individual trials with replacement and repeating the identical analysis procedure on each new dataset. CIs of the peak inducer durations producing maximal forward jumps and maximal forward mislocalization completely excluded each other: peak forward mislocalization was observed at 21 ms (95% CI = 8–27 ms) whereas peak forward jumps was observed at 71 ms (95% CI = 60–80 ms). This strongly suggests that motion and position judgments are maximally affected by the High-Phi illusion at different inducer durations.

A repeated-measures ANOVA was conducted to verify the effect of inducer duration on jump direction and position shift magnitude. For Jump trials, Mauchly's Test of Sphericity (Mauchly, 1940) indicated that the assumption of sphericity was not met ($\chi^2(230) = 563.1$, $P < 0.001$). Therefore, ANOVA results will be reported with Greenhouse-Geisser correction (1959). A significant main effect of inducer duration was found ($F(21,609) = 25.5$, $P < 0.001$, $\eta^2_{\text{partial}} = 0.47$). In Position trials, the assumption of sphericity was also violated ($\chi^2(230) = 687.5$, $P < 0.001$). With the Greenhouse-Geisser correction, a significant main effect of inducer duration was found ($F(21,609) = 20.2$, $P < 0.001$, $\eta^2_{\text{partial}} = 0.41$).

Overall, Experiment 1 shows that the High-Phi illusion not only induces an illusory motion signal (that is, a perceived jump forward or backward), but also influences the perceived position of concurrently presented objects. Furthermore, both motion and position judgments showed a biphasic pattern of dependence on inducer duration, with short inducer durations leading to perceived jumps and mislocalization in the direction of the inducer, and longer inducer durations leading to perceived jumps and mislocalization in the opposite direction. However, motion and position judgments were maximally

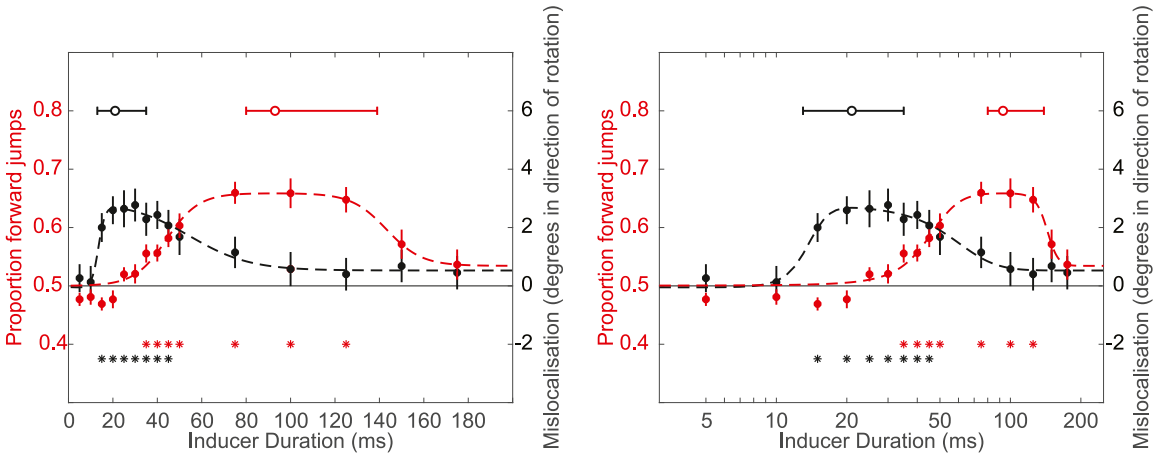

Figure 3. Results Experiment 2. Red markers indicate the proportion of jumps reported in the direction of inducer motion in Jump trials (left vertical axis), and black markers indicate the mean mislocalization in the direction of motion on Position trials (right vertical axis). Identical datapoints are plotted on linear (left panel) and logarithmic (right panel) abscissas. Asterisks below the plots indicate inducer durations where datapoints are significantly different from zero (two-tailed *t*-test, $P < 0.05$, Bonferroni corrected). Datapoints are fitted with double-logistic functions (dashed lines) and the inducer durations at which these functions are maximal are indicated with filled circles above the plots. Horizontal lines extending from these circles indicate bootstrapped 95% confidence intervals, indicating that as in Experiment 1, the High-Phi illusion maximally influenced perceived motion and position at different inducer durations.

induced in the forward direction at different inducer durations, with maximum forward mislocalization evident at shorter inducer durations than maximum forward jumps.

Experiment 2

We carried out a second experiment in order to replicate our original finding, and to further investigate the different inducer durations leading to maximal forward jumps and mislocalization. Experiment 2 therefore mirrored Experiment 1, with the exception that we tested a more fine-grained set of short inducer durations. To increase the power of our statistical tests, we also obtained more trials per inducer duration.

Methods

All methods in Experiment 2 are identical to Experiment 1, with the following exceptions:

Twenty-one observers (15 women and 6 men) took part in this experiment, aged between 19 and 33 years (M = 22.71, SD = 3.15). None of the observers had previously participated in Experiment 1. Inclusion criteria were otherwise identical to Experiment 1.

Stimuli were identical to Experiment 1, with the exception that we tested a different range of inducer durations (5, 10, 15, 20, 25, 30, 35, 40, 45, 50, 75, 100, 125, 150, and 175 ms). Each of the 15 inducer durations was presented 12 times per block, for a total of 180 trials per block. Observers completed five Jump blocks followed by five Position blocks.

Results

Mean proportion of forward jumps (in the Jump trials) and mean mislocalization (in the Position trials) were calculated as a function of inducer duration as in Experiment 1. Results for both Jump and Position blocks are shown in Figure 3. As before, data are shown on both linear (left panel) and logarithmic abscissas (right panel). The pattern of results replicates the findings of Experiment 1, with both trial types characterized by forward jumps / mislocalization at short inducer durations.

As before, we tested the proportion of perceived jumps and mean mislocalization against zero at each individual time point, correcting for multiple comparisons by Bonferroni correction. The results reveal a significant pattern of forward jumps at inducer durations from 25 to 125 ms, and significant forward mislocalization at inducer durations of 15 to 45 ms. This pattern of the High-Phi illusion inducing forward shifts in position at shorter inducer durations than forward jumps is consistent with our results from Experiment 1.

As in Experiment 1, we investigated the different dependence on inducer duration more formally by fitting double logistic functions to the observed data (indicated as dashed lines in Figure 3), and taking the peak of the fitted functions as the inducer

duration at which we observed maximal forward jumps c.q. maximal forward mislocalization. We calculated bootstrapped 95% CIs of these estimates in the same way as in Experiment 1, and, as before, these convincingly demonstrated that the two effects peak at different inducer durations: peak forward mislocalization was observed at 21 ms (95% CI = 13–35 ms), and peak forward jumps was observed at 93 ms (95% CI = 80–139 ms).

A repeated-measures ANOVA was conducted to verify the effect of inducer duration on jump direction and position shift magnitude. For Jump trials, Mauchly's Test of Sphericity indicated a departure from the assumption of sphericity ($\chi^2(104) = 151.9$, $P = 0.002$). Therefore, ANOVA results will be reported with Greenhouse-Geisser correction. A significant main effect of inducer duration was found ($F(14,280) = 16.0$, $P < 0.001$, $\eta^2_{partial} = 0.44$). In Position trials, the assumption of sphericity was also violated ($\chi^2(104) = 190.3$, $P < 0.001$). With the Greenhouse-Geisser correction, a significant main effect of inducer duration was found ($F(14,280) = 6.48$, $P < 0.001$, $\eta^2_{partial} = 0.24$).

Altogether, Experiment 2 convincingly replicates all observations from Experiment 1: we observe both a significant proportion of forward jumps as well as significant forward mislocalization, and these two judgments are maximally affected at different inducer durations.

Experiment 3

Finally, we carried out a third experiment to investigate the effect of inducer speed on jumps and position shifts, as, if these effects are due to extrapolation along the motion trajectory, we would expect that a higher speed would increase the magnitude of jumps or position shifts. In this experiment, the number of inducer durations was reduced, but we included several different speeds, spanning from previously investigated values (Wexler et al., 2013) to the speed used in Experiments 1 and 2. Additionally, we measured jump magnitude with a continuous response, so this could be compared with the magnitude of position shifts, and balanced the order of experiments within observers.

Methods

All methods in Experiment 3 are identical to previous experiments, with the following exceptions:

Eight observers (5 women and 3 men, including author P.J.) aged between 22 and 31 years (M = 25.38, SD = 3.42) took part in this experiment. None of the observers had previously participated in Experiments 1 or 2. Inclusion criteria were identical to Experiment 1.

Due to restrictions on in-person testing due to coronavirus disease 2019 (COVID-19), observers completed the experiment from their own homes. All observers still used an ASUS ROG PG258 monitor (ASUS, Taipei, Taiwan) with a resolution of 1920 × 1080 running at 200 Hz, and completed the experiment in a quiet, dimly lit room. Observers did not use a chinrest but were instructed to sit approximately 50 cm from the screen with the fixation point at eye level.

Stimuli were identical to previous experiments, but each of the seven transients were presented for only 5 ms each, whereas in Position trials the flash was on-screen for 15 ms, spanning three transient frames. The range of inducer durations was changed (5, 10, 20, 40, 80, 160, and 320 ms), and inducer speed was manipulated, with the inducer rotating at 12.5, 25, 50, 100, or 200 degrees rotation/s. Each combination of inducer duration and speed was repeated 18 times in each session, over two sessions. Trials were randomly shuffled within tasks and sessions, and split into three blocks.

In Jump blocks, rather than a 2 AFC, observers now reported the magnitude of the jump angle by moving the mouse horizontally right or left, corresponding to a clockwise or counter-clockwise jump, respectively. This changed the size of a corresponding black wedge on the screen. Observers clicked to submit their response when the angle of the wedge matched the size of the perceived jump. The jump magnitude for each condition was calculated by averaging the reported signed angles. The proportion of forward jumps was calculated by converting the reported angle into a binary value of forward or backward with respect to the preceding motion, excluding trials in which no jump was reported (a magnitude of 0 degrees).

The experiment was split into two sessions lasting 1 hour. In the first session, half of the observers completed three Jump blocks, followed by three Position blocks, whereas the other half completed the blocks in the opposite order. This was reversed in the second session, such that every observer completed one session with Jump blocks first and one with Position blocks first.

Results

Mean proportion of forward jumps and mean magnitude of jumps (in the Jump trials) and mean mislocalization (in the Position trials) were calculated as a function of inducer duration and inducer speed. Results are shown in Figure 4. As the jump magnitude was recorded in this experiment, rather than just direction, it is possible to qualitatively compare the size of the jump to the size of the corresponding position

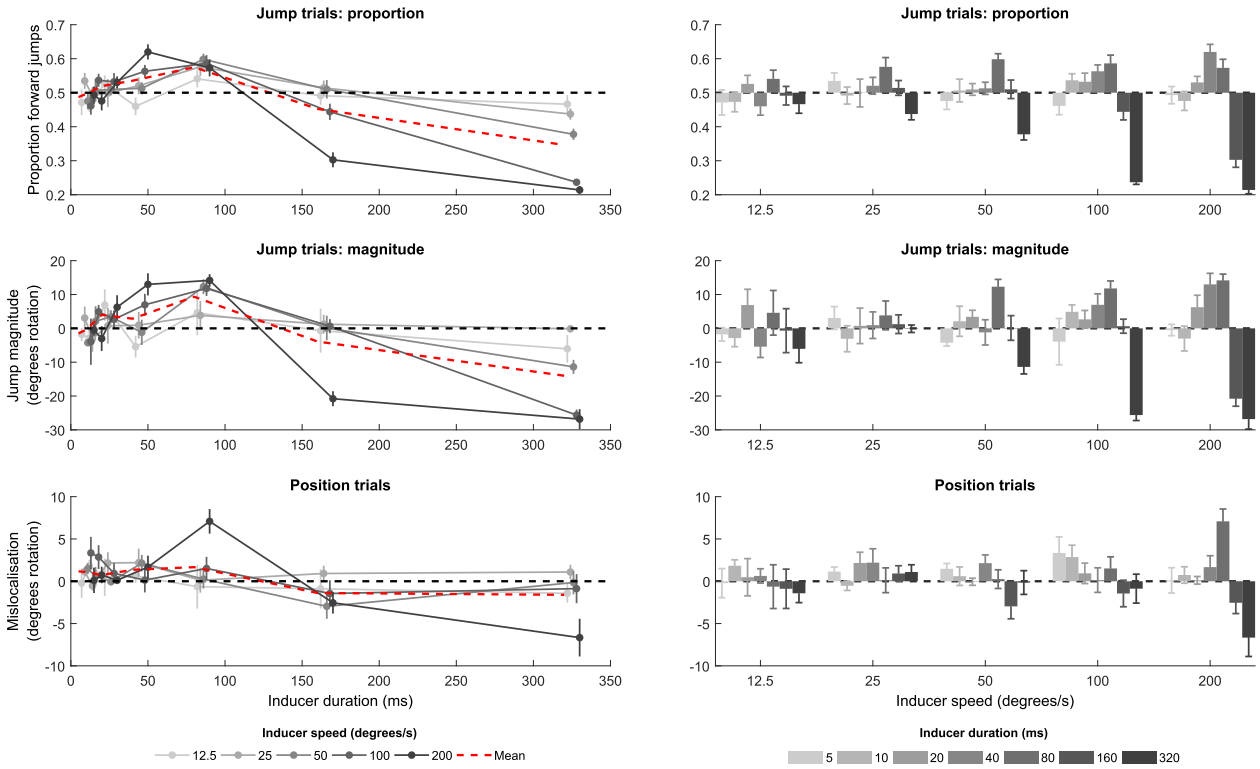

Figure 4. Results Experiment 3. Left panels: proportion forward jumps (top), jump magnitude (middle), and mislocalisation magnitude (bottom) plotted as a function of inducer duration, separately for each inducer speed. Red dotted lines show the mean across all inducer speed. Right panels: the same data plotted as a function of inducer speed, separately for each inducer duration. Error bars show standard error of the mean. As in Experiments 1 and 2, jumps and position shifts appear to be forward at short inducer durations and backward at longer inducer durations. Additionally, this response scales with inducer speed, such that faster speeds appear to lead to a higher proportion of forward and backward jumps, as well as jumps and mislocalizations of a larger magnitude.

shift. Consistent with previous literature (Cavanagh & Anstis, 2013; Wexler et al., 2013) mislocalizations were generally found to have a considerably smaller magnitude than jumps, at the same inducer duration and speed.

In this experiment, because we tested fewer inducer durations, we could not robustly fit logistic functions. Instead, to investigate the effect of inducer speed on jumps and position shifts, we investigated how the mean dependence on inducer duration scaled with speed. To do so, we first averaged responses at each inducer duration across all observers and inducer speeds, giving three functions which characterize the effect of inducer duration on the variable of interest (proportion forward jumps, jump magnitude, or position shift magnitude). These mean functions are plotted on Figure 4 (left panels) as red, dotted lines. Within observers, we fit these mean functions to the response to each inducer speed separately (grey lines in Figure 4, left panel) by allowing each mean function to scale in magnitude. A scaling factor larger than one will change the shape of the function by making the positive and negative peaks larger, indicating a larger effect of inducer speed, whereas a scaling factor smaller than one will flatten function, indicating a smaller effect of inducer speed. This gave us a measure of the effect of inducer speed on the direction and magnitude of jumps and position shift. Results from individual observers and mean results can be seen plotted on Figure 5. Qualitatively, it can be seen that for all observers and dependent variables, the scaling factor increases in size with increasing inducer speed. In order to quantify this relationship, a linear mixed effects model was fit for each independent variable (proportion forward jumps, jump magnitude, and mislocalization magnitude), with scaling factor as the dependent variable. These models included a fixed effect of inducer speed and a fixed intercept, as well as a random slope and intercept for each individual observer. The parameter of interest is the fixed slope, as this shows the effect of inducer speed on the scaling factor, controlling for variability across individual observers. Likelihood ratio tests were used to compare a null model, which did not include a fixed effect of inducer speed, to each full model. The full models were significantly better than the null model across all measurements. For Jump trials, looking first at proportion of forward jumps, the fixed effect of inducer speed was 0.009 (95% CIs = 0.005–0.013;

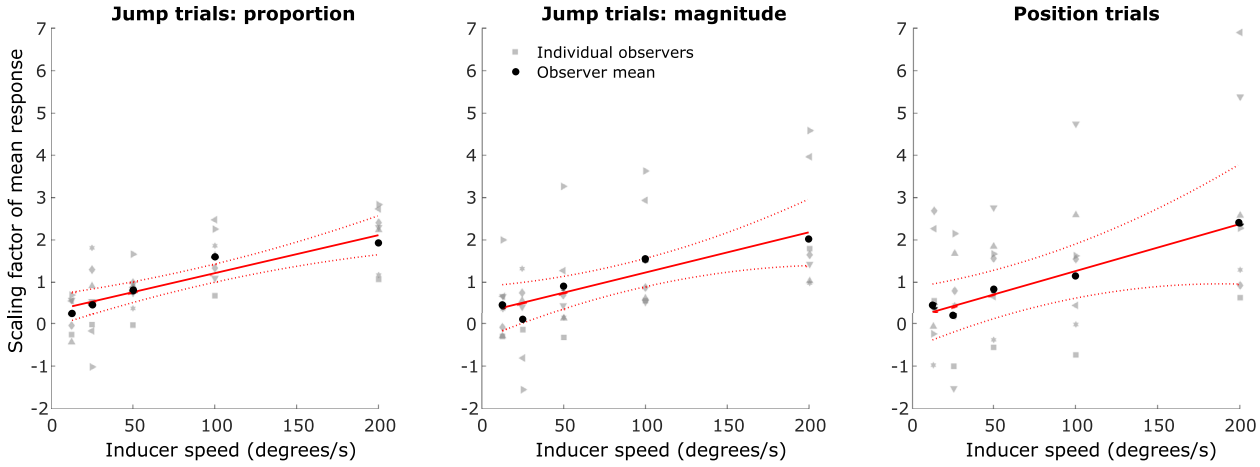

Figure 5. Effect of inducer speed on proportion of forward jumps (left panel), jump magnitude (central panel) and mislocalization (right panel). First, a mean function was calculated across all observers and all inducer speeds (shown as red dotted lines in Figure 4, left panels). This overall mean was scaled to fit individual observer responses, over each inducer speed, allowing the overall mean to scale linearly. This gives a scaling factor of the mean response (y-axis) for each inducer speed (x-axis). Results of this fit for individual observers are plotted as grey points, with different marker shapes for each observer, while the means for each inducer speed across all observers are plotted as black circles. A linear mixed effects model was fit for each measurement type, including a fixed effect of inducer speed (plotted in red with 95% confidence intervals). For all measurement types the gradient of this fit was approximately 0.01 ($P < 0.05$), indicating that the proportion of forward jumps, jump magnitude, and mislocalization magnitude scale with inducer speed.

$\chi^2(1) = 11.64$, $P = 0.0006$). Taking jump magnitude as the independent variable, the fixed effect of inducer speed was 0.010 (95% CIs = 0.003–0.016; $\chi^2(1) = 6.39$, $P = 0.01$). For Position trials, the fixed effect of inducer speed was 0.011 (95% CIs = 0.002–0.020; $\chi^2(1) = 4.58$, $P = 0.03$). These results show that as inducer speed increases, the proportion of forward jumps, jump magnitude, and position shift magnitude scales proportionally, at close to the same rate across the different measurements.

To verify our interpretation of these results, we carried out a 3-way repeated measures ANOVA for each of the three dependent measures, with three within-subject factors: task order (whether the task was completed first or second within one session), inducer duration and inducer speed. The sample size is too small to detect departures from sphericity (Field, Miles & Field, 2012), therefore, the results of the ANOVA will be reported with and without the Greenhouse-Geisser correction, which is the most conservative correction available.

For Jump trials, taking the proportion of forward jumps as the dependent variable, inducer duration had a significant effect ($F(6,42) = 18.81$, $P < 0.001$ with and without correction, $\eta^2_{\text{partial}} = 0.73$). No other main effects were significant. A significant interaction effect was found between inducer duration and inducer speed ($F(24,168) = 4.10$, $P < 0.001$ without correction, $P = 0.007$ with correction, $\eta^2_{\text{partial}} = 0.37$).

Inducer duration also had a significant effect on the magnitude of the jump in the High-Phi effect ($F(6,42) = 10.85$, $P < 0.001$ without correction, $P = 0.002$ with correction, $\eta^2_{\text{partial}} = 0.61$). Additionally, the interaction effect between inducer duration and inducer speed was significant without correction ($F(24,168) = 3.31$, $P < 0.001$, $\eta^2_{\text{partial}} = 0.32$), but not significant with correction ($P = 0.06$).

For Position trials, the inducer duration had a significant effect on the magnitude of the position shift without correction ($F(6,42) = 2.89$, $P = 0.02$, $\eta^2_{\text{partial}} = 0.29$), but this was no longer significant with correction ($P = 0.07$). Again, the interaction effect between inducer duration and inducer speed was significant without correction ($F(24,168) = 1.76$, $P = 0.02$, $\eta^2_{\text{partial}} = 0.20$), but not significant with correction ($P = 0.18$).

Discussion

The High-Phi illusion is a striking visual illusion in which replacing a moving texture with a new, static texture creates a strong illusion of visual motion (Wexler et al., 2013). Here, we investigate the hypothesis that this illusion is caused by the same motion extrapolation mechanisms that have been argued to underlie a range of other motion-position illusions, including the flash-lag effect. In three experiments, we

presented observers with a High-Phi stimulus, and asked them to either report the direction in which they perceived an illusory jump, or to localize a target that was briefly flashed concurrently with the new texture. We observed that the High-Phi illusion not only causes an illusory motion percept, as previously reported, but also shifts the perceived position of concurrently presented objects. Furthermore, perceived position shifts depended on inducer duration in a similar way to illusory jumps: we observed short inducer durations to cause forward jumps and position shifts, and longer durations to cause backward jumps and position shifts. We further demonstrated that these effects scaled with inducer speed. Importantly, however, peak effects on position and motion were dissociable: we observed maximum forward shifts in position at shorter inducer durations than maximum forward jumps.

The High-Phi illusion therefore has analogous, speed-dependent effects on both position and motion, but with subtly different time courses. We believe the most parsimonious explanation for this is that the High-Phi illusion is caused by an interplay of predictive motion extrapolation and postdictive corrective mechanisms (Eagleman, 2008): predictive motion extrapolation mechanisms cause the forward jump and position shift at short inducer durations (e.g. Nijhawan 2008; Burkitt & Hogendoorn preprint), and postdictive correction-for-extrapolation mechanisms cause the backward jump and position shift at longer inducer durations (e.g. Blom et al., 2019; Shi & Nijhawan, 2012). As faster moving objects should be extrapolated further forward and corrected further backward along their motion path, we further corroborated this explanation by demonstrating that faster inducer speeds lead to larger forward and backward jumps and positions shifts. Consistent with previous findings, we observed that illusory jumps were substantially larger than illusory position shifts, but this is unsurprising because judgments of position are based on a physically presented stimulus, whereas judgments of jump magnitude are based solely on spurious correlations between random textures. So how might this be implemented at the neural level?

At short inducer durations, the onset of the moving texture rapidly generates a motion signal in the early visual system (Westheimer & McKee, 1977). This accompanies the early afferent position signal, forming a population code that represents both position and velocity, as proposed by previous theoretical (Hogendoorn & Burkitt, 2019) and computational studies (Khoei, Masson, & Perrinet, 2017; Kwon, Tadin, & Knill, 2015). These models predict that this visual motion signal causes a shift in the receptive fields of downstream neural populations in the direction opposite to the direction of motion – a prediction consistent with fMRI evidence (Harvey & Dumoulin, 2016; Liu, Ashida, Smith, & Wandell, 2006; Maus, Fischer, & Whitney, 2013; Schneider et al., 2019; Whitney et al., 2003). As a result, subsequent incoming neural signals are processed as if they originated from a position further along the trajectory, leading to a shift in the perceived position of the briefly flashed object. Such a mechanism would effectively extrapolate moving objects along their trajectory, and, in addition to possibly playing a role in compensating for neural transmission delays (Nijhawan, 2002; Nijhawan, 2008), it would explain the forward position shift observed here at short inducer durations.

With regard to the perceived forward jump caused by the High-Phi illusion at short inducer durations, Wexler and colleagues argue that the visual transient caused by the presentation of the new texture amplifies a preceding motion "seed" (Wexler et al., 2013, p. 7080). At short inducer durations, this "seed" is the motion signal caused by the inducer, causing a sharp illusory jump in the same direction. What the precise mechanism is behind this amplification is not entirely clear. Because the two textures are high contrast and uncorrelated, the transient contains substantial motion energy in all directions; one possibility is that the interpretation of this (non-direction selective) motion energy is primed or biased by the inducer. This is reminiscent of the motion-bridging effect (Mattler & Fendrich, 2007), in which motion too fast to be consciously perceived can nevertheless bias the perceived direction of a subsequently presented bistable apparent motion sequence. This interpretation is also consistent with models of predictive coding in the visual cortex (e.g. Rao & Ballard, 1999) and with the emerging understanding that expectations (either neural or cognitive) shape perception (de Lange, Heilbron, & Kok, 2018). Furthermore, because these neural predictions most likely require feedback connections from higher areas (Hogendoorn & Burkitt, 2019; Kok, Bains, Van Mourik, Norris, & De Lange, 2016), it makes sense that longer inducer sequences are required to induce illusory forward jumps than illusory position shifts (which, as outlined above, are caused by changes to the faster afferent pathway).

At longer inducer durations, we observe that the High-Phi illusion reverses, such that the transient induces both jumps and position shifts in the backward direction. Wexler et al. (2013) similarly observed backward jumps after long inducer durations, and argued that the motion "seed" that causes these jumps arises from motion adaptation. Although adaptation to motion is more frequently thought of as taking place on a time-scale of multiple seconds (causing a motion aftereffect; Anstis, Verstraten, & Mather, 1998), neural adaptation to motion has been shown to start after motion stimuli as brief as 25 ms (Glasser, Tsui, Pack, & Tadin, 2011). This study showed that even after sub-second duration motion sequences, subsequently presented stationary stimuli evoked direction-selective

responses in macaque motion area MT, particularly at short inter-stimulus intervals. Moreover, these adapting sequences can produce measurable directional perceptual after-effects, even if they are themselves so short that their own motion direction cannot be perceived (Glasser et al., 2011). These observations fit with our results, in that we observe a progressive reduction in the forward position shift starting at inducer durations around 20 to 30 ms. This shift continues to reduce as adaptation accumulates, ultimately becoming a backward shift for inducers longer than ~ 100 to 500 ms. Importantly, Glasser et al. argue that their MT results are inherited from earlier upstream regions, such that the origin of this rapid neural adaptation lies in the very early visual system. For instance, they show that adaptation at least partly takes place before binocular integration (an observation that parallels what is observed in the flash-grab illusion; van Heusden et al., 2019). Taken together, the evidence is consistent with the proposal that long inducer durations cause rapid neural adaptation in early visual areas, such that the subsequently presented static texture causes a brief, strong motion signal in the opposite direction. This motion signal then affects downstream receptive fields, and consequently the perceived position of the concurrently presented flash, in exactly the same way as outlined above for brief pulses of real motion. Finally, we suggested above that forward jumps might be observed at longer inducer durations than forward shifts because position shifts result from rapid changes in afferent receptive fields, whereas consolidating the motion percept likely requires additional cortical feedback connections. In the same way, we might speculate that the effects of adaptation are evident more rapidly in the afferent pathways that subserve perceived position than in the feedback networks putatively involved in the illusory motion percept, but this is a hypothesis that will need further research.

The present study diverges from Wexler et al.'s previous findings in demonstrating that the magnitude of the High-Phi jump is dependent on the speed of the inducer (as is the position shift). Wexler et al. proposed that the illusory jump corresponds to a jump with maximum detectable velocity, however, our findings contradict this, as we show that the same inducer duration causes a larger jump when the inducer is rotating faster. It is possible this result emerged because a broader range of speeds were tested in the present study, ranging from 12.5 to 200 degrees rotation/second as opposed to 10 to 30 degrees rotation/second used by Wexler et al. Additionally, inducer durations of 3 to 5 seconds were used by Wexler et al. when manipulating inducer speed, which is much larger than the inducer durations used in Experiment 3 here (5–320 ms). It is possible that, after a long inducer, the effect of speed asymptotes to a maximum, as described by Wexler et al. In order to resolve these discrepancies, future experiments should explore a wider range of inducer speeds and durations.

Functionally, this rapid low-level neural motion adaptation and the resulting jerk backward along the direction of motion has the effect of undoing the forward shifts caused by previous extrapolation processes. In so doing, this mechanism effectively corrects for overextrapolation, as initially proposed by Nijhawan and colleagues in the context of the flash-lag effect (Maus & Nijhawan, 2006; Maus & Nijhawan, 2008; Nijhawan, 2008; Shi & Nijhawan, 2012) and also reported in the flash-grab effect (Blom et al., 2019). Interestingly, these findings emphasize the role of the transient in triggering the correction; when the transient is rendered invisible, overextrapolation is observed. In this context, it is again interesting to compare the High-Phi illusion with the motion bridging effect, in that the circular array of dots rotating too fast to be consciously perceived as motion nevertheless causes a subsequently presented static array of dots to seem to "spin to a halt" (Stein, Fendrich, & Mattler, 2019) in the same direction as the original display. Because the speed of the dots significantly exceeds the upper limit for motion adaptation (Verstraten, Van Der Smagt, & Van De Grind, 1998), the transient does not induce a motion signal in the opposite direction, no corrective mechanism is triggered and the dots spin to a halt in the forward, rather than backward direction. We argue that the transient in the High-Phi illusion therefore neatly reveals two complementary neural mechanisms for localizing moving objects: extrapolation for short inducer durations, and correction-for-extrapolation for longer inducer durations.

There is abundant neural evidence for the existence of motion extrapolation mechanisms in the early visual system. This includes motion extrapolation mechanisms in the retinae of mice, salamanders, and rabbits (Berry et al., 1999; Schwartz et al., 2007), cat LGN (Sillito, Jones, Gerstein, & West, 1994) and both cat (Jancke, Erlhagen, Schöner, & Dinse, 2004) and macaque V1 (Subramaniyan et al., 2018). Comparable mechanisms have been reported in humans on the basis of EEG (Blom, Feuerriegel, Johnson, Bode, & Hogendoorn, 2020; Hogendoorn & Burkitt, 2018; Johnson, Blom, Feuerriegel, Bode, & Hogendoorn, 2019) and fMRI evidence (Ekman, Kok, & de Lange, 2017; Schellekens, van Wezel, Petridou, Ramsey, & Raemaekers, 2016; see Hogendoorn, 2020 for a review). The current findings are consistent with these neural mechanisms and provide further insight into the perceptual consequences of those mechanisms. Furthermore, our findings demonstrate that the High-Phi illusion might be a fruitful paradigm for future studies to probe the time-course of extrapolation mechanisms specifically and motion-position interactions more generally.

Keywords: High-Phi, extrapolation, motion, position, illusion

Acknowledgments

P.J., S.D., and H.H. were supported by the Australian Government through the Australian Research Council's Discovery Projects funding scheme (project DP180102268).

Commercial relationships: none.
Corresponding author: Philippa Johnson.
Email: pajohnson@student.unimelb.edu.au.
Address: Melbourne School of Psychological Sciences, Redmond Barry Building, University of Melbourne, Tin Alley, Parkville, Victoria, Melbourne 3010, Australia.

References

Anstis, S. M. (1989). Kinetic edges become displaced, segregated, and invisible. In D. Lam (Ed.), *Neural mechanisms of visual perception* (Vol. *2*, pp. 247–260). Houston, TX: Gulf Publishing.

Anstis, S. M., Verstraten, F. A., & Mather, G. (1998). The motion aftereffect. *Trends in Cognitive Sciences, 2*(3), 111–117.

Berry, M. J., Brivanlou, I. H., Jordan, T. A., & Meister, M. (1999). Anticipation of moving stimuli by the retina. *Nature, 398*(6725), 334–338.

Blom, T., Feuerriegel, D., Johnson, P., Bode, S., & Hogendoorn, H. (2020). Predictions drive neural representations of visual events ahead of incoming sensory information. *Proceedings of the National Academy of Sciences, 117*(13), 7510–7515.

Blom, T., Liang, Q., & Hogendoorn, H. (2019). When predictions fail: Correction for extrapolation in the flash-grab effect. *Journal of Vision, 19*(2), 1–11.

Brainard, D. H. (1997). The Psychophysics Toolbox. *Spatial Vision, 10*(4), 433–436.

Cai, R. H., & Schlag, J. (2001). Asynchronous feature binding and the flash-lag illusion. *Investigative Ophthalmology and Visual Science, 42*(4), Abstract S711.

Cavanagh, P., & Anstis, S. M. (2013). The flash grab effect. *Vision Research, 91*, 8–20.

de Lange, F. P., Heilbron, M., & Kok, P. (2018). How do expectations shape perception? *Trends in Cognitive Sciences, 22*(9), 764–779.

De Valois, R. L., & De Valois, K. K. (1991). Vernier acuity with stationary moving Gabors. *Vision Research, 31*(9), 1619–1626.

Eagleman, D. M. (2008, April 14). Prediction and postdiction: Two frameworks with the goal of delay compensation. *Behavioral and Brain Sciences*. Cambridge, England, UK: Cambridge University Press.

Eagleman, D. M., & Sejnowski, T. J. (2000). Motion integration and postdiction in visual awareness. *Science (New York, N.Y.), 287*(5460), 2036–2038.

Eagleman, D. M., & Sejnowski, T. J. (2007). Motion signals bias localization judgments: A unified explanation for the flash-lag, flash-drag, flash-jump, and Frohlich illusions. *Journal of Vision, 7*(4), 3.

Ekman, M., Kok, P., & de Lange, F. P. (2017). Time-compressed preplay of anticipated events in human primary visual cortex. *Nature Communications, 8*, 15276.

Fabius, J. H., Fracasso, A., Nijboer, T. C. W., & Van der Stigchel, S. (2019). Time course of spatiotopic updating across saccades. *Proceedings of the National Academy of Sciences of the United States of America, 116*(6), 2027–2032.

Fabius, J. H., Fracasso, A., & Van der Stigchel, S. (2016). Spatiotopic updating facilitates perception immediately after saccades. *Scientific Reports, 6*, 34488.

Field, A., Miles, J., & Field, Z. (2012). *Discovering statistics using R*. Thousand Oaks, CA, USA: Sage Publications.

Fröhlich, F. W. (1924). Über die Messung der Empfindungszeit. *Pflügers Archiv Für Die Gesamte Physiologie Des Menschen Und Der Tiere, 202*(1), 566–572.

Glasser, D. M., Tsui, J. M. G., Pack, C. C., & Tadin, D. (2011). Perceptual and neural consequences of rapid motion adaptation. *Proceedings of the National Academy of Sciences of the United States of America, 108*(45) E1080–E1088.

Greenhouse, S. W., & Geisser, S. (1959). On methods in the analysis of profile data. *Psychometrika, 24*(2), 95–112.

Harvey, B. M., & Dumoulin, S. O. (2016). Visual motion transforms visual space representations similarly throughout the human visual hierarchy. *Neuroimage, 127*, 173–185.

Hogendoorn, H. (2020). Motion extrapolation in visual processing: Lessons from 25 years of flash-lag debate. *Journal of Neuroscience, 40*(30), 5698–5705.

Hogendoorn, H., & Burkitt, A. N. (2018). Predictive coding of visual object position ahead of moving objects revealed by time-resolved EEG decoding. *NeuroImage, 171*, 55–61.

Hogendoorn, H., & Burkitt, A. N. (2019). Predictive coding with neural transmission delays: a real-time

temporal alignment hypothesis. *Eneuro, 6*(April), ENEURO.0412–18.2019.

Hogendoorn, H., Verstraten, F. A. J., & Cavanagh, P. (2015). Strikingly rapid neural basis of motion-induced position shifts revealed by high temporal-resolution EEG pattern classification. *Vision Research, 113*(Pt A), 1–10.

Hosoya, T., Baccus, S. A., & Meister, M. (2005). Dynamic predictive coding by the retina. *Nature, 436*(7047), 71–77.

Hubbard, T. L. (2014). The flash-lag effect and related mislocalizations: Findings, properties, and theories. *Psychological Bulletin*. *140*(1), 308–338.

Jancke, D., Erlhagen, W., Schöner, G., & Dinse, H. R. (2004). Shorter latencies for motion trajectories than for flashes in population responses of cat primary visual cortex. *Journal of Physiology, 556*(3), 971–982.

Johnson, P., Blom, T., Feuerriegel, D., Bode, S., & Hogendoorn, H. (2019). 2019. In *Proceedings of the Australasian Cognitive Neuroscience Society*.

Kanai, R., & Verstraten, F. A. (2005). Perceptual manifestations of fast neural plasticity: Motion priming, rapid motion aftereffect and perceptual sensitization. *Vision Research, 45*(25-26), 3109–3116.

Khoei, M. A., Masson, G. S., & Perrinet, L. U. (2017). The flash-lag effect as a motion-based predictive shift. *PLOS Computational Biology, 13*(1), e1005068.

Kok, P., Bains, L. J., Van Mourik, T., Norris, D. G., & De Lange, F. P. (2016). Selective activation of the deep layers of the human primary visual cortex by top-down feedback. *Current Biology, 26*(3) 371–376.

Kwon, O.-S., Tadin, D., & Knill, D. C. (2015). Unifying account of visual motion and position perception. *Proceedings of the National Academy of Sciences of the United States of America, 112*(26), 8142–8147.

Liu, J. V., Ashida, H., Smith, A. T., & Wandell, B. A. (2006). Assessment of stimulus-induced changes in human V1 visual field maps. *Journal of Neurophysiology, 96*(6), 3398–3408.

Mattler, U., & Fendrich, R. (2007). Priming by motion too rapid to be consciously seen. *Perception & Psychophysics, 69*(8), 1389–1398.

Mauchly, J. W. (1940). Significance test for sphericity of a normal n-variate distribution. *The Annals of Mathematical Statistics, 11*(2), 204–209.

Maus, G. W., Fischer, J., & Whitney, D. (2013). Motion-dependent representation of space in area MT+. *Neuron, 78*(3), 554–562.

Maus, G. W., Khurana, B., & Nijhawan, R. (2010). History and theory of flash-lag: past, present, and future. In R. Nijhawan, & B. Khurana (Eds.), *Space and Time in Perception and Action* (pp. 477–500). Cambridge, London, UK: Cambridge University Press.

Maus, G. W., & Nijhawan, R. (2006). Forward displacements of fading objects in motion: The role of transient signals in perceiving position. *Vision Research, 46*(26), 4375–4381.

Maus, G. W., & Nijhawan, R. (2008). Motion extrapolation into the blind spot. *Psychological Science, 19*(11), 1087–1091.

Maus, G. W., & Nijhawan, R. (2009). Going, going, gone: Localizing abrupt offsets of moving objects. *Journal of Experimental Phychology, Human Perception and Performance, 35*(3), 611–626.

Nijhawan, R. (1994). Motion extrapolation in catching. *Nature*. *370*(6487), 256–257.

Nijhawan, R. (2002). Neural delays, visual motion and the flash-lag effect. *Trends in Cognitive Sciences, 6*(9), 387.

Nijhawan, R. (2008). Visual prediction: Psychophysics and neurophysiology of compensation for time delays. *Behavioral and Brain Sciences, 31*(2), 179–239.

Pinkus, A., & Pantle, A. (1997). Probing visual motion signals with a priming paradigm. *Vision Research, 37*(5), 541–552.

Priebe, N. J., Churchland, M. M., & Lisberger, S. G. (2002). Constraints on the source of short-term motion adaptation in macaque area MT. I. The role of input and intrinsic mechanisms. *Journal of Neurophysiology, 88*(1), 354–369.

Ramachandran, V. S., & Anstis, S. M. (1990). Illusory displacement of equiluminous kinetic edges. *Perception, 19*(5), 611–616.

Rao, R. P. N., & Ballard, D. H. (1999). Predictive coding in the visual cortex: A functional interpretation of some extra-classical receptive-field effects. *Nature Neuroscience, 2*(1), 79–87.

Schellekens, W., van Wezel, R. J. A., Petridou, N., Ramsey, N. F., & Raemaekers, M. (2016). Predictive coding for motion stimuli in human early visual cortex. *Brain Structure and Function, 221*(2), 879–890.

Schneider, M., Marquardt, I., Sengupta, S., Martino, F. De, & Goebel, R. (2019). Motion displaces population receptive fields in the direction opposite to motion. *BioRxiv*, 759183. Retrieved from https://www.biorxiv.org/content/10.1101/759183v2.

Schwartz, G., Taylor, S., Fisher, C., Harris, R., & Berry, M. J. (2007). Synchronized firing among retinal ganglion cells signals motion reversal. *Neuron, 55*(6), 958–969.

Shi, Z., & Nijhawan, R. (2012). Motion extrapolation in the central fovea. *PLoS One, 7*(3), 33651.

Sillito, A. M., Jones, H. E., Gerstein, G. L., & West, D. C. (1994). Feature-linked synchronization of thalamic relay cell firing induced by feedback from the visual cortex. *Nature, 369*(6480), 479–482.

Sinico, M., Parovel, G., Casco, C., & Anstis, S. (2009). Perceived shrinkage of motion paths. *Journal of Experimental Psychology: Human Perception and Performance, 35*(4), 948–957.

Stein, M., Fendrich, R., & Mattler, U. (2019). Stimulus dependencies of an illusory motion: Investigations of the motion bridging effect. *Journal of Vision, 19*(5), 1–23.

Subramaniyan, M., Ecker, A. S., Patel, S. S., Cotton, R. J., Bethge, M., & Pitkow, X. et al. (2018). Faster processing of moving compared with flashed bars in awake macaque V1 provides a neural correlate of the flash lag illusion. *Journal of Neurophysiology, 120*(5), 2430–2452.

van Heusden, E., Harris, A. M., Garrido, M. I., & Hogendoorn, H. (2019). Predictive coding of visual motion in both monocular and binocular human visual processing. *Journal of Vision, 19*(1), 3.

Verstraten, F. A. J., Van Der Smagt, M. J., & Van De Grind, W. A. (1998). Aftereffect of high-speed motion. *Perception, 27*(9), 1055–1066.

Westheimer, G., & McKee, S. P. (1977). Spatial configurations for visual hyperacuity. *Vision Research, 17*(8), 941–947.

Wexler, M., Glennerster, A., Cavanagh, P., Ito, H., & Seno, T. (2013). Default perception of high-speed motion. *Proceedings of the National Academy of Sciences of the United States of America, 110*(17), 7080–7085.

Whitney, D., & Cavanagh, P. (2000). Motion distorts visual space: shifting the perceived position of remote stationary objects. *Nature Neuroscience, 3*(9), 954–959.

Whitney, D., Goltz, H. C., Thomas, C. G., Gati, J. S., Menon, R. S., & Goodale, M. A. (2003). Flexible retinotopy: motion-dependent position coding in the visual cortex. *Science, 302*(5646), 878–881.